The complex interplay of lead halide perovskites with their surroundings

*Juan F. Galisteo-López, Mauricio E. Calvo, Hernán Míguez**

Instituto de Ciencia de Materiales de Sevilla (Consejo Superior de Investigaciones Científicas-Universidad de Sevilla). C/Américo Vespucio 49, 41092 Sevilla (Spain).

Keywords: lead halide perovskites, photophysics, structural defects

Abstract:

Photoexcitation of lead halide perovskites induces a restructuration of the material that simultaneously enhances its emission properties and triggers its degradation. These concomitant processes are strongly dependent on the surroundings of the perovskite, both while and after being processed, underlining the relevance the environment and the interfacial design has in the stability and performance of these materials and the devices based on them. This shocking observation reveals that when subjected to external illumination, lead halide perovskites undergo a number of photophysical processes that strongly modify their structure and thus their optoelectronic properties. Such photoinduced instability stems from a defective structure directly linked to the low temperature and solution processed fabrication routes generally employed to build perovskite solar cells with efficiencies comparable to state-of-the-art values. On the other hand, these same inexpensive and unsophisticated procedures make this material a promising component in energy conversion devices. In this *Progress Report* we analyze the different impact on the perovskite structure, hence on its optoelectronic performance, that the interaction with its surroundings has, providing specific examples that highlight this interplay, describing the kind of modification it induces, and listing

the related effects on the optoelectronic properties that should be accounted for when characterizing them.

1. Introduction:

Lead-halide perovskites (LHPs) are materials with the general formula ABX_3 where A is a monovalent cation (methylammonium, formamidinium, cesium, rubidium or a combination of them), B a bivalent metallic cation (lead or tin) and X a halide anion (chlorine, bromine, iodine or a combination of them). [1] LHPs have become one of the most technologically relevant materials of the first two decades of the 21st century due to their stunning performance in optoelectronic applications and, in particular, in photovoltaic (PV) devices essential for the needed paradigm change in energy production. [2] LHPs have also been successfully incorporated into light emitting devices, [3] photodetectors [4] and showed potential for lasing applications.[5] For the case of PV devices, such outstanding performance stems from properties such as their strong broadband absorption, low exciton binding energy [6] and long carrier diffusion lengths in excess of the typical absorbing layer thickness. [7] Adding to this, a key ingredient in their success is the possibility of solution processing this material at low temperature from earth abundant constituents. Further, the option of modifying its composition provides extra degrees of freedom affecting their electronic bandgap but also its stability. [8]

But, in spite of all these advantages, when studying the optoelectronic properties of LHPs one usually faces the issue of comparing results from different samples prepared under seemingly identical conditions, with nominally the same composition, and yet showing different optoelectronic properties, be they light harvesting efficiency, photoluminescence quantum yield or charge transport.[9] This strong variability hides a

rich phenomenology inherent to this type of materials that is heavily affected by a complex interplay with the atmosphere in which they are synthesized, processed or measured, as well as with the adjacent materials to which they are coupled (i.e., charge transporting or injecting layers) in order to make a device. To simplify, we will refer to the environment and the interfaces of the perovskite as the "surroundings".

In this Progress Report we shall deal with the optoelectronic properties of LHP films and their interaction with the surroundings, which, as we will see, is likely behind the processes that play a key role on their outstanding performance and, paradoxically, also constitutes their main weakness. The phenomenology of the above interactions, and its prevalence in LHPs regardless of their exact composition or morphology, points to the universality of these processes. Finally, means to prevent or exploit these interactions having in mind the final industrial application of these materials are revised.

2. A perovskite is a perovskite and its circumstance: External factors determining the optoelectronic performance of LHP films

Let us start by describing a revealing observation: when the photoluminescence (PL) of a solution processed LHP thin film, kept and transported in both an oxygen (O_2) and water (H_2O) free atmosphere, is measured under vacuum, the semiconductor behaves as a poor emitter [10,11,12] or, in other words, as one with a low PL external quantum yield, η_{ext}, defined as the ratio between emitted and absorbed photons. Being LHPs direct bandgap semiconductors, this effect can be attributed either to many-body non-radiative Auger recombination or to the presence of a large number of non-radiative decay paths associated with defects in the crystalline network. As such low quantum yield is observed even for excitation densities for which Auger processes are negligible,

[13] lattice defects are clear candidates to be behind this behavior. On the other hand, when the same film is exposed to low levels of molecular oxygen (O_2), the PL intensity raises abruptly several orders of magnitude. [14,15,12,16]. This enhancement in PL intensity, which is observed for LHP having different compositions and morphologies, is accompanied invariably by changes in the recombination dynamics of photogenerated carriers. In particular upon exposure to the combined action of light and an oxygen-rich atmosphere, charge carrier recombination is slowed down as evidenced from time-resolved PL measurements [10,11,15] further pointing to a reduction in non-radiative recombination channels.

Now, as the difference between the actual open circuit voltage attained from a solar cell, V_{OC}, and the maximum ideal one, V_{OC}^{*}, is given by: [17]

$$V_{OC} - V_{OC}^{*} = k_B T \ln \eta_{ext} \qquad (1)$$

, where k_B stands for the Boltzmann constant and T for temperature, it follows that approaching the optimized performance of a single-junction solar cell demands not only a good absorbing material but also one with $\eta_{\mathrm{ext}} \approx 1$ under open circuit conditions. Equation (1) basically states that any generic good photovoltaic material must also be a good light emitter.[18] Hence the peculiar response of LHPs to O_2 exposure mentioned above not only provides clear evidence of the conspicuous interplay of LHPs with the environment, but also has profound implications regarding their use as photovoltaic materials, as it indicates that interaction with the environment (or, as we will see later, adjacent materials) will determine the performance of any LHP-based device. In the following sections we will discuss what types of defects are more likely to affect the optoelectronic performance of LHP and how this influence is modified by the interactions that occur between the perovskite and its surroundings.

2.1. Defects affecting the optoelectronic performance of perovskites

For LHPs, and in particular the archetypal methyl ammonium lead iodide $MAPbI_3$, the intrinsic maximum theoretical efficiency for a solar cell (30.5%) is close to the Shockley-Queisser (SQ) limit. [19] Thus, structural defects represent one of the main limitations for future improvements in photo-conversion efficiency. Due to the low-temperature solution processing of these materials, which constitute one of the main advantages from the point of view of their transition into an industrial application, large defect densities are anticipated. Interestingly, state-of-the art defect densities reported for single crystals (10^9-$10^{10}cm^{-3}$) [20,21,22] and thin films (10^{14}-$10^{16}cm^{-3}$) [23,24,25] of LHP with different composition are rather high but do not prevent LHP-based devices from performances close to those of commercial devices, pointing to the acknowledged defect tolerant character of these materials.

Regarding the nature of defects affecting the performance of an LHP-based device, recent theoretical reports indicate that, while not having the lowest formation energy, halide interstitials in $MAPbX_3$ (X=Br or I) could be responsible for the introduction of deep trap levels within the bandgap (**Figure 1a**) acting as non-radiative recombination centers within the bulk.[26] Defects can also form at the crystal surface and grain boundaries in polycrystalline films compromising their optoelectronic properties. In this direction, many passivation strategies have been implemented to reduce non-radiative recombination at grain surfaces on polycrystalline films by using either small molecules (Lewis bases or acids) or inorganic layers.[23,27,28,29] A reduction in defect density close to an order of magnitude has been reported, reflecting in an enhanced PL as well as improved PV performance.

Several spectroscopic studies have found evidence of the presence of structural defects according to the above numerical simulations [26] but unveiling their precise nature and

spatial distribution is a non-trivial task. Nevertheless, while an exact picture of the defect landscape in LHPs is currently missing, impressive work in determining the nature and spatial distribution of structural defects within LHPs has appeared recently. A multimodal correlative approach involving compositional, structural and electronic information pointed to hole trap clustering at grain surfaces being responsible for PL quenching in triple cation LHPs similar to those holding the photo conversion efficiency (PCE) record (**Figure 1b**) [30]. Further, the leading role of surfaces in introducing deep-traps for a variety of material morphologies was demonstrated using drive-level capacitance profiling. [31] But structural disorder in LHP polycrystalline films, routinely used in the best performing PV devices, is not limited to the single grain level. A more complex picture has been recently revealed [32] where a multi-scale disorder scenario takes place comprising strain patterns within and across crystalline grains (**Figure 1c**). This strain was correlated with material emission and thus device performance. The above results evidence the complex defect structure of LHPs fabricated by means of solution process methods and points to further experimental work needed in the future to precisely characterize it.

Regarding inorganic LHP with the general formula $CsPbX_3$, several theoretical studies have been also carried out pointing towards a defect tolerant system. [33,34] In these materials defects introducing deep trap levels within the electronic bandgap, mostly antisites, have large formation energies and are thus expected to be scarce. For these LHP the particular case of the grain surface has been considered pointing to halide interstitials as playing a key role as charge traps. [35] Calculations have also been carried out for finite sized nanocrystals where most probable defects are located at the surface and lead to the formation of deep traps only when surface ligands are removed.

[36] Such defect chemistry is likely responsible for the outstanding QY attained for inorganic LHP NCs when appropriate surface ligands are used. [37]

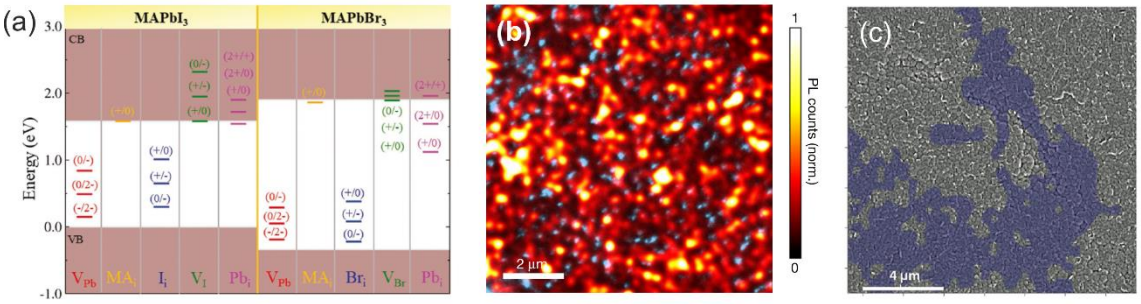

Figure 1. (a) Density Functional Theory (DFT) simulations of thermodynamic ionization levels for the most stable defects in $MAPbI_3$ and $MAPbBr_3$. (b) Over imposed images of a PL map (color plot) and trap clusters mapped by photoemission electron microscopy (blue dots) in a $(Cs_{0.05}FA_{0.78}MA_{0.17})Pb(I_{0.83}Br_{0.17})_3$ film. (c) Quiver plot over imposed on an SEM image of an $(MA_{0.15}\ FA_{0.79}Cs_{0.06})Pb(I_{0.85}Br_{0.15})_3$ film evidencing the presence of long-range strain patterns extending beyond the single-grain level. Reproduced with permission (a) [26] Copyright 2019 Wiley, (b) [30] Copyright 2020 Springer Nature, (c) [32] Copyright 2019 Royal Society of Chemistry.

2.2. Photoinduced ion migration

When irradiated with continuous wave illumination or a pulsed light source with high yield, LHPs undergo drastic changes in their optoelectronic performance, which comprise PL enhancements, decays or a succession of the two (see above). Such changes take place over time scales of seconds to minutes, much longer than those involved in carrier transport or recombination, pointing at slower processes such as ion migration [38] as responsible for them. Further, these variations, in the absence of any change in the absorption, are indicative of a change in the balance between radiative and non-radiative recombination processes and thus of the defect density within the material. Observed in the early stages of the field [39,40] these changes in PL are associated with the phenomenon of light soaking where the PCE of a PV device undergoes an improvement upon exposure to external illumination. Such PCE

improvement can be correlated with the PL changes further indicating a reduction in non-radiative recombination. [40] This indicates that point defects, apart from introducing non-radiative recombination paths for photoexcited carriers, represent migration routes for the ions constituting the perovskite lattice.

When studied by means of micro-PL techniques, LHP samples consistently present an inhomogeneous spatial distribution of their emission. [15,23,41,42,43,44,45,46,47] Such emissive spatial pattern undergoes a strong redistribution when the above mentioned macroscopic PL activation/depletion takes place, irrespective of material composition and morphology (albeit both affect the magnitude and dynamics of the PL changes). These studies have provided relevant information helping to shed some light on the nature of photoinduced emissive changes. The correlation of initially dark/bright microscopic regions in a sample with the PL activation rate (**Figure 2a and 2b**) [41,45,46] or changes in locally probed PL lifetimes (**Figure 2c-e**) [41,42,45,46] allowed associating this phenomenology with the presence of crystalline defects and their passivation. Further, correlative microscopy studies providing local information on PL and composition established a connection between halide-related defects and ionic migration. [41,43] In this direction, the light-induced migration of the halide species has been shown to eventually lead to material degradation upon prolonged irradiation (**Figure 2f-i**). [43,48]

While the ultimate mechanism behind these photoinduced changes is still lacking, the key role played by structural disorder is now acknowledged. This effect can thus be mitigated upon appropriate passivation of crystalline defects and in particular those located at surfaces and grain boundaries. [23,27,28,29] The role of bulk halide-related defects has also been shown to play a relevant role in the PL enhancement, and associated with the annihilation of halide-related Frenkel pairs. [49] Finally, an

additional means to prevent photoinduced changes comprises acting on other factors affecting ionic migration within the lattice. This includes compositional engineering, in particular for the A-site cation, where an appropriate choice of ions has led to the most stable materials and devices. [50] The origin of such instability is likely a combination of a higher defect formation energy in these systems [51] and a higher migration energy barrier for ions as a result of small lattice distortions introduced by the use of a combination of cations. [52]

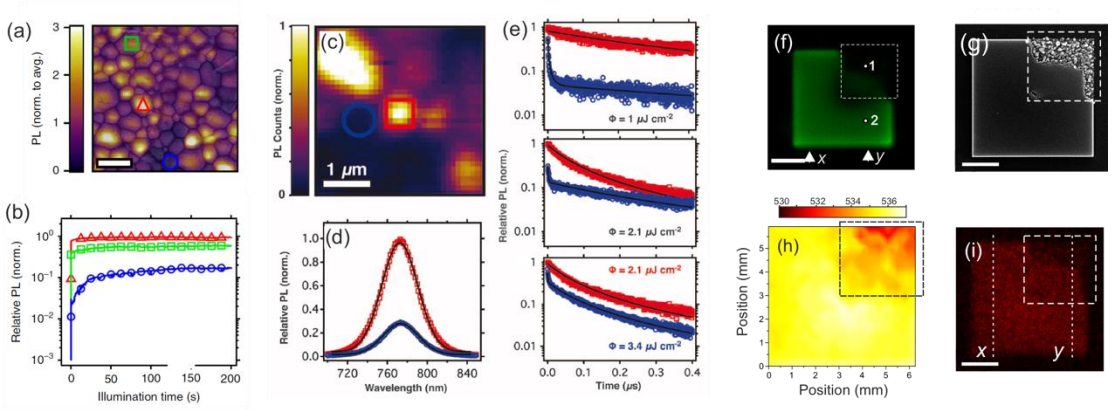

Figure 2. (a) micro PL image from a $MAPbI_3$ film (scale bar is 2μm) and (b) evolution of PL with time as the sample is illuminated from the three different regions highlighted in (a). (c) micro-PL image from a $MAPbI_3$ film comprising dark and bright regions. (d) PL spectra and (e) PL decay curves at different excitation fluences from dark and bright regions. (f) PL image from a $MAPbBr_3$ platelet after prolonged irradiation of a region highlighted by a dashed line (scale bar is 1μm). SEM image (g), spectral (h) and EDX compositional map corresponding to Br (i) for the same platelet. Reproduced with permission (a), (b) [41] Copyright 2016 Springer Nature, (c), (d), (e) [2342] Copyright 2015 American Association for the Advancement of Science, (f), (g), (h), (i) [43] Copyright 2016 American Chemical Society.

The above mentioned photo-induced halide redistribution within the perovskite lattice is likely behind other phenomena such as the ubiquitous phase segregation reported for mixed-halide perovskites (mLHP). [53] The latter involves the formation of sample regions with different halide composition upon exposure to external irradiation. This constitutes a limitation for PV operation, where the formation of phases with different

bandgap leads to a drop in efficiency, [54] but also for emission applications where material stability compromises its spectral characteristics. A vast amount of literature has appeared over the past few years presenting evidence that link this photo-induced phenomenon with aspects such as sample morphology, [55,56,57,58] stoichiometry [59] or defect structure [60,61,62,63,64,65]. All these influence ionic migration in these materials and thus acting on them represent the main means to overcome this issue. [66]

2.3. Interplay between structural defects and the surrounding atmosphere

In inorganic semiconductors the adsorption of O_2 and H_2O on its surface, which can be further aided by external illumination, is known to cause a bending of energy bands which will influence the performance of an optoelectronic device. [67] For the case of LHP, the interaction with these two molecular species has been shown to induce a number of structural changes which drastically affect the efficiency and durability of this material. In particular, the long term exposure of LHPs to O_2 is known to contribute to their degradation, [68,69] leading to an irreversible drop in device performance. These effects are not restricted to the surface as it has been proposed that oxygen species can propagate through the lattice into the bulk (**Figure 3a**) and enter I-related vacancies [70] or interstitial sites. [71] Regarding the role of water, while the presence of small amounts during the synthesis of $MAPbI_3$ can favor nucleation and growth leading to samples having a better crystalline quality and improved device performance, an excessive amount can induce its degradation. [72] Such degradation strongly depends upon the termination of the $MAPbI_3$ structure where methylammonium (MA) terminated surfaces undergo a rapid solvation process in the presence of H_2O molecules leading to the desorption of the MA component. [73] This process can be further accelerated in the presence of external illumination, something that has been attributed

to the photostriction effect observed in LHP that could favor the penetration of H_2O molecules within the perovskite lattice. [74]

But the interaction of H_2O and O_2 with the LHP lattice can also have beneficial effects as it has been demonstrated that these molecular species play a key role in the above-mentioned photobrightening, [75] a phenomenon that has greatly puzzled researchers over the past few years. The role of the surrounding atmosphere was initially observed for LHP of different compositions [10,11,14,15] where the presence of O_2 led to the above mentioned enhanced PL while an inert atmosphere caused a reversible drop in the emission (see **Figure 3b-c**). Such variations in PL efficiency pointed to the creation/annihilation of non-radiative recombination paths induced by the combined presence of light and atmosphere and were expected to have a direct incidence in the performance of LHP-based devices. A vast amount of experimental and theoretical evidence has been provided over the past few years that point to a number of complex mechanisms behind these changes. Many of the mechanisms invoked to account for such PL enhancement involve the formation of superoxide species. These can act as passivating agents for structural defects comprising halide vacancies (**Figure 3d**) [76,45,46,77,78] or create a negatively charged surface layer that induces the migration of halide ions leading to the recombination of interstitial/vacancy pairs. [12] Other mechanisms which have been shown to contribute comprise the passivation of halide interstitials by changing its oxidation state (**Figure 3e**) [79] and the passivation of surface metallic lead Pb^0 by H_2O_2, [80] further evidencing the complexity of the interaction between the LHP and its surrounding atmosphere. As for H_2O, its presence in combination with external irradiation has also been demonstrated to lead to an improvement in the emission from LHP that can reflect in improved device performance

and stability. [45,46] Here a partial degradation of the LHP surface can lead to the formation of an amorphous layer that passivates surface traps.

As many of the above mentioned mechanisms dealing with oxygen-induced photobrightening involve the presence of superoxide species, as it was the case for degradation, a plausible scenario is one where both processes coexist, and thus the prevalence of one or the other is just a matter of the duration of the irradiation. [12] The coexistence of both processes has also been suggested for the particular case of $MAPbI_3$ where, as a consequence of the annihilation of halide-related Frenkel pairs, I_2 can form and diffuse to the surface where it acts as an electron trap. [26] As for the case of unintentional disorder, it has been proposed [75] that this PL instability could be used to improve the optoelectronic performance of LHP by irradiating the sample for as long as enhancement dominates the photo-induced changes and protecting it to avoid the latter degradation stage.

Remarkably, the relevance of the surrounding atmosphere during the synthesis and processing of the materials constituting a LHP device has been demonstrated just recently. [81] When exposed to humid air conditions, $MAPbI_3$ behaves as an intrinsic semiconductor. This situation is modified when the material is subjected to high vacuum conditions which removes adsorbed superoxide and hydrated species leading to the re-appearance of shallow traps and a strong n-doping of the material. This implies that O_2 and H_2O, which have been proposed as passivating agents of halide vacancies [45,46,78] and responsible for the introduction of shallow traps, [26] may also contribute to effectively doping the material and thus altering the energy level landscape of the device.

While most of the above results deal with the popular formulations $MAPbBr_3$ and $MAPbI_3$ being the ones used most extensively in devices, the emergence of new

material configurations (mixed-halide perovskites, all-inorganic perovskites, 2D perovskites, etc.) has risen the question as to how these new materials are affected by the atmosphere. To this date only a few reports have been presented indicating that also for these novel materials the interaction with their immediate surroundings are likely to play a key role in the performance of future devices.

All-inorganic lead-halide perovskites (iLHP) have demonstrated potential as efficient light emitters to be incorporated into LEDs in the shape of nanocrystals and in recent years, also in PV devices with efficiencies reaching certified values above 18%. [82] One key advantage of iLHP is the enhanced stability in the absence of organic moieties within the perovskite lattice. This fact also influences its interaction with oxygen as degradation related with this gas is absent and only defect passivation is expected to take place. In this direction, the introduction of atomic oxygen in halide vacancies present in the bulk was shown to improve the emitting properties of $CsPbI_2Br$ films accompanied by a rise in the PV performance of devices made from them. [83] Using oxygen as a passivating agent could then be used in the future to further rise state of the art PV efficiencies. [82] But beyond bulk defects, O_2 has also been demonstrated to act as a passivating agent for Pb-rich surface defects which act as PL scavenger in iLHP nanostructures, [84,85] pointing to future passivating strategies that do not rely on the use of organic ligands that could compromise charge transport in devices.

2D LHP, with enhanced stability as a result of reduced moisture-induced degradation [86] and halide migration [87] due to the presence of large organic spacers between the inorganic layers, have also demonstrated an improvement in their emission in the presence of an oxygen rich atmosphere. [88] While the ultimate mechanism in these low-dimensional structures still remains to be unveiled, in part due to the lack of detailed reports on the nature of crystalline defects in these systems, an experimental

evidence that mimics that of their 3D counterparts points again to the passivation of traps.

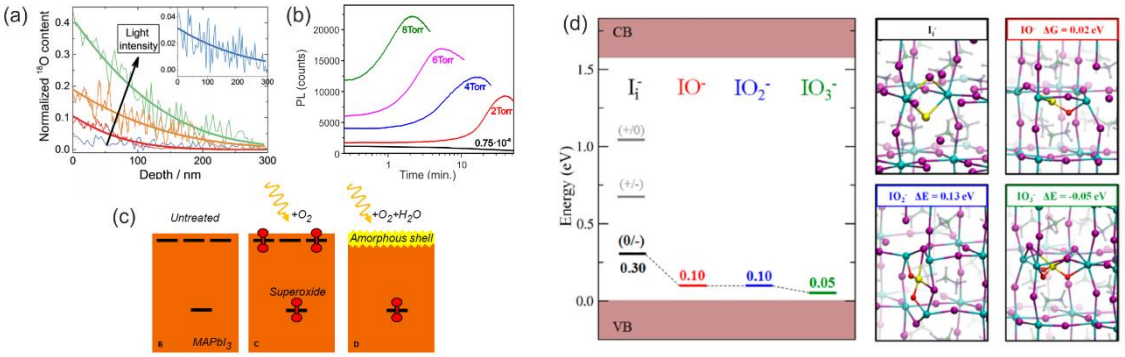

Figure 3. (a) Experimental evidence for the light-aided introduction of oxygen within the bulk of a $MAPbI_3$ lattice. (b) Dependence of the PL of $MAPbBr_3$ thin films on the surrounding environment. (c) Scheme illustrating the passivation of defects associated with halide vacancies in $MAPbI_3$ by means of superoxide and the combined presence of oxygen and moisture. (d) Evolution of the energy as a function of its change in oxidation state for defect states associated with the presence of iodide interstitials in $MAPbI_3$. Reproduced with permission (a) [71] Copyright 2018 Royal Society of Chemistry, (b) [12] Copyright 2018 American Chemical Society, (c) [46] Copyright 2018 Wiley and (d) [79] Copyright 2017 American Chemical Society.

2.4. Interplay with adjacent materials

For a LHP film in a device, the primary interaction front that has to be considered, provided a proper isolation from the surrounding atmosphere is achieved, are charge transporting layers (CTLs) [89]. When choosing the appropriate CTLs, suitable energy levels to selectively extract photogenerated carriers and high carrier mobility are usually considered. But the reactivity with the CTL interface needs to be considered as it critically determines both the device efficiency as well as its long-term stability. Regarding device efficiency, CTLs can be designed as a means to passivate surface defects. In this direction some examples comprise the use of Lewis bases that were employed as electron-transporting layers (ETLs) with the potential to passivate positively charged surface traps, improving the device performance (**Figure 4a-c**).

[27,90,91] In an analogous manner, Lewis acids can act as electron acceptors which effectively passivate defects and act as hole-transporting layer (HTLs). [92,93] Furthermore, O_2 induced degradation reactions, leading to the efficiency drop of LHP solar cells, can thus be prevented by the use of interlayers that efficiently remove surface charges before they react with O_2. [94,95]

But the interaction with adjacent CTLs can have the opposite effect and contribute to the degradation of the device, thus leading to an irreversible efficiency loss. Examples of interaction between the CTLs and the LHP layer abound. One key aspect is the above-mentioned halide migration which can lead to the formation of charge barriers as a result of the reaction between the halide and metal electrodes. [96,97] Electrode degradation can also arise from the interaction with volatile residues from LHP light-induced degradation, and could be prevented by choosing the appropriate ETL acting as an encapsulating layer. [98] Ionic migration can take place also from metallic (Au) electrodes through ETL leading to the formation of shunt paths. [99] Further, the LHP film itself can degrade upon reaction with adjacent CTLs. Oxidation at the interface with TiO_2 [100] or proton-transfer reactions at the LHP/ZnO interfaces [101] can lead to LHP irreversible degradation. All this implies that in the choice for an appropriate CTL, beyond energetic and charge transport aspects, the interaction with the LHP film will need to be considered in order to reduce material degradation of the different device components. In carefully choosing the different interfaces comprising a device impressive gain in in its durability can be achieved [102,103] pointing to interface engineering as a critical aspect of LHP-based device fabrication.

An example which clearly evidences the relevance of the interaction of LHP with its surroundings is that of the detrimental role of UV radiation on the performance of LHP-based solar cells. Here the combined presence of light and oxygen determines the

interaction of the adjacent layers with the LHP film. As we move into the UV range of the EM spectrum different processes take place that affect both the LHP layer as well as other layers comprising an optoelectronic device, compromising its performance. The role of UV irradiation on device performance was already pointed out in the early stages of the field [104] and associated with the presence of TiO_2, one of the most commonly used ETL, where oxygen vacancies in the TiO_2 layer act as traps for photoinduced electrons. In order to minimize these effects several approaches have been proposed spanning from removing UV radiation altogether using spectral filters to the substitution of TiO_2 with alternative ETL materials such as other metal oxide layers [104,105], fullerenes [106] and surface-modified TiO_2 [107] On the other hand, the effect of UV irradiation on the LHP material itself could be another source of degradation that has not been thoroughly studied.

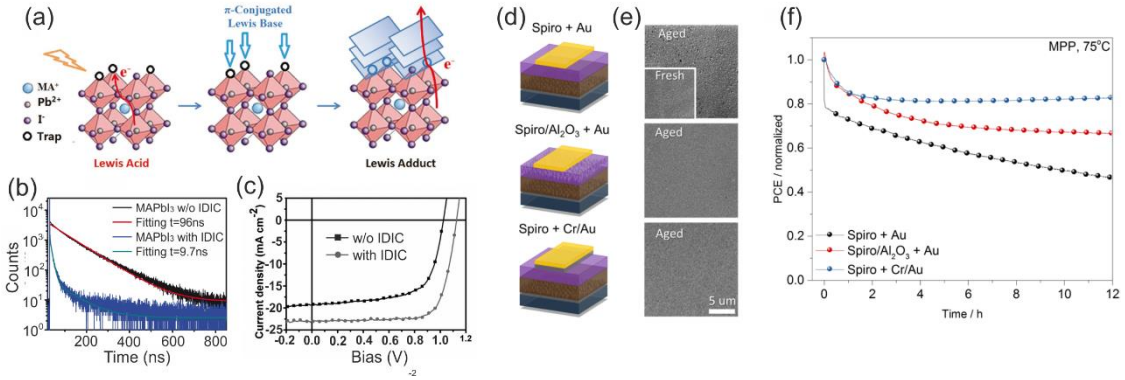

Figure 4. (a) Diagram of Lewis acid (as a consequence of under-coordinated surface Pb atoms) passivation with a π-conjugated Lewis base indacenodithiophene end-capped with 1.1-dicyanomethylene-3-indanone (IDIC). (b) PL decay curves of an isolated $MAPbI_3$ film and one contacted with IDIC. (c) J-V curves of devices with and without an IDIC layer. Device schemes (d), corresponding SEM images (e) and time-evolution PCE (f) illustrating the use of Cr layers to prevent Au diffusion from electrodes and corresponding device degradation. Reproduced with permission (a), (b), (c) [90] Copyright 2017, Wiley, (e), (f) Copyright 2016 [99] American Chemical Society.

2.5. Relation between synthesis conditions and environmental sensitivity

One of the advantages of the synthesis of standard LHP thin films by solution processing is the possibility to add stabilizing compounds. The liquid face preparation also allows controlled modification of the stoichiometry of ABX_3 perovskites, which has a very significant impact on the eventual sensitivity of the material to environmental conditions. In either of these ways, interaction with the surroundings can be rationally tackled. A paradigmatic example is the strong influence that the modification of the lead/halide ($Pb:X^-$) or lead/A cation ($Pb:A^+$) ratios have on the grain boundaries and the perovskite crystal quality.[108] In the case of hybrid inorganic-organic LHP, under-stoichiometric Pb causes the accumulation of organic compounds at the interfaces that hinders the inter-grain charge transport.[109] On the other hand, an excess of Pb in the precursor leads to a PbI_2 layer that could improve the efficiency of a LHP solar cell due to the reduction of ionic migration and, in consequence, the hysteresis of the I/V curve.[110] However, experiments based on time resolved fluorescence and transient absorption spectroscopy demonstrate the most important effect of the PbI_2 layer is the passivation of defects at the grain boundaries which is traduced in a low density of non-radiative recombination centers.[111,112] This type of PbI_2 self-induced passivation layer can also be a consequence of the different degradation pathways that perovskite suffers when they are exposed to ambient conditions. **Figure 5a** shows photocurrent and PL color maps that are obtained when the surface of LHP was intentionally degrade to form PbI_2 In that case, it was demonstrated that the PbI_2 layer resulting from a controlled degradation of LHP perovskite must be thinner than 20nm to enhance the performance of the treated solar cell.[113] The formation of thicker layers is detrimental for the charge carrier transport due to the insulating character of PbI_2. (**Figure 5b**).

Additionally, the use of a sub-stoichiometric amount of lead (X/Pb > 3) prevents the formation of metallic lead centers which act as charge carrier traps.

The concept of a passivating layer obtained through the adding of proper perovskite precursors is also applied for the enhancement of the luminescent (and electroluminescent) response of the LHP layer. For this purpose, a core shell $CsPbBr_3$@MABr structure (MABr, methylammonium bromide) was achieved based on the different crystallization rates of both compounds involved.[114] $CsPbBr_3$ precursors are mixed together with an excess of MABr. During the film formation, the MABr crystallization occurs after that the $CsPbBr_3$ due to their differences in solubility. **Figure 5c** reveals the surrounding layer of MABr that fills the voids between LHP crystals in an $CsPbBr_3$ film. MABr not only passivates the traps that prevents the radiative recombination in the inorganic perovskite film but also balances the charge injection when the $CsPbBr_3$@MABr film is integrated as the active layer in a lighting emission device.

In a different approach, inorganic KI was added directly in the precursor solution. The effect of this addition is the neutralization of halide vacancies in a sort of passivation layer that decorates the LHP grain boundaries.[115] From that way, ionic drift is limited leading to increase in efficiency and stability of photovoltaic devices that incorporates KI.

Reversely, the strong dependence of the optoelectronic properties with the synthesis conditions reveal that LHPs are also extraordinarily sensitive to the microenvironment in which it takes place. In fact, the intentionally use of an excess of reactants, with respect to the concentrations that would correspond to the exact stoichiometry, may lead to an accumulation of unreacted precursors, which will affect the interaction of the newly formed LHP with its surroundings. For instance, changes in both concentration or

reaction time not only yields modifications in the stoichiometry, but also gives rise to the presence of PbI_2 or AX in the fresh film.[109] Furthermore, grain boundaries films can also trap solvent vapors and they are affected more than other part of the microstructure to thermal, mechanical and light stresses. Initial efforts to protect *in situ* with a continuous medium were dedicated to the use of polymers. It was shown that this type of compounds can be added directly to the LHP precursor solution to reduce the crystal size or to modify the crystalline phase in MAPI films.[116] A careful selection among the myriad of polymers has distinguished the use of triblock copolymers with hydrophobic hydrophilic moieties.[117] In **Figure 5d**, it can be observed the effect of the polymer on the ground boundaries and a scheme of how the polymer functionalizes perovskite surface. In this case, photovoltaic devices prepared with this compound leaded to stabilized high efficient photovoltaic devices.

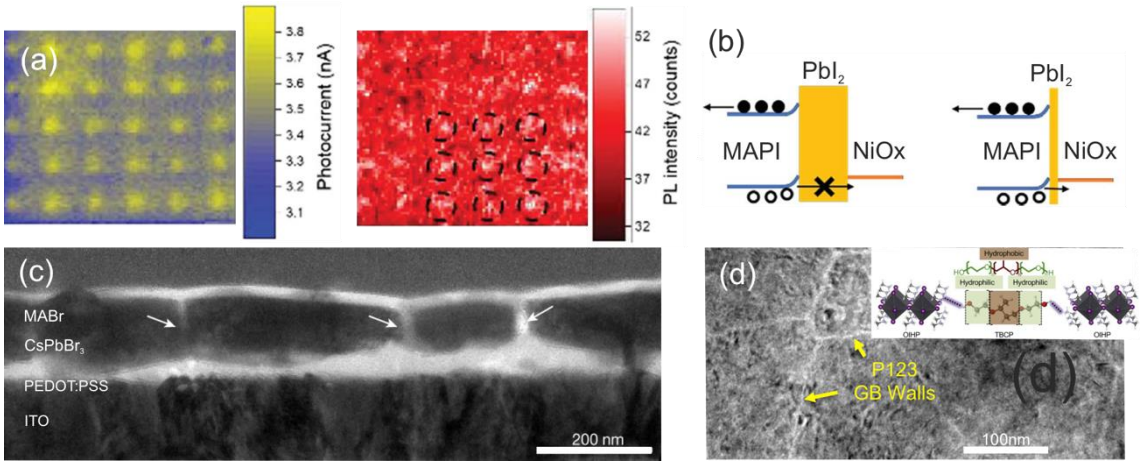

Figure 5. (a) Spatial distribution of photocurrent (left) and PL (right) of perovskite device degraded to PbI_2 (20nm) in air with laser. Scale of each magnitude is represented at the side of each graph. (b) Scheme of the electronic mechanism that operates under a thin (left) or a thick (right) PbI_2 layer. (c) Cross-section electron microscopy image of $CsPbB_3$ layer (gray regions) deposited on top of PEDOT:PSS in presence of excess of MABr (represented by the bright region). Arrows indicate the presence of MABr between $CsPbBr_3$ crystals. (d) Electronic microscopy top view of a MAPI film deposited in the presence of a tri-block copolymer (P123). Bright regions correspond to P123 surrounding grain boundaries. Inset: scheme of the functionalization obtained with the polymer. Reproduced with permission (a),(b) [113] Copyright 2018, Royal Soc. Chemistry, (c) [114] Copyright 2018, Springer Nature, (d) [117] Copyright 2018, Elsevier Inc.

2.6. Interplay of LHPs with electric fields

Besides the dependence of the LHPs response on the chemical environment or the radiation to which they are exposed, for most applications, be they related to light harvesting or emission, these materials are also subjected to electric fields, which might be externally applied or internally generated as a result of different photophysical processes. The soft nature of LHP also implies that significant structural modifications may be induced by these fields and, in fact, a wide variety of effects resulting from the interaction of LHP with them has been reported. One of the most significant effects of applied electric fields is, as it occurs under photoexcitation, ion migration, as it has been demonstrated by temperature dependent dark current decay measurements.[118]Indeed, A cations or halide anions are prone to migrate due to the low activation energy this process demands. In general, this charge drift produces instabilities under the normal operation of LHP solar cells, generating macroscopic charged regions,[119] and thus a non-uniform distribution of the electric fields in the perovskite layer, which negatively affects the photocurrent generation. On the other hand, ion migration can also be useful to heal defects in the LHP lattice, as it has been recently shown. Indeed, control over the applied voltage and thus over ion migration may result in the passivation of defects in the LHP, which enhances the performance and the stability of the LHP solar cell.[120]

Beyond the effect on ion migration, and as mentioned before, illumination of a LHP layer integrated in a solar device also produces an internal electric field as consequence of spatial separation of electrons and holes. Under these circumstances, external applied voltages could modify the response of the charge carriers. At short circuit (SC) the (built-in) internal electric field and current density are the highest, whereas at open circuit (OC) the charge flow balance is null, the external potential equally opposes to the internal, and ions accumulate at the interfaces. For this reason, degradation of LHP

solar cell is highly dependent on the operation conditions, being faster at OC than at SC[121] and minimized at the voltage corresponding to the maximum power conversion efficiency of the device.[122]

The effect of the electric field applied on a LHP layer also affects to the spatial distribution and the intensity of the photoluminescence. When voltage is applied, the photoluminescence in LHP drops almost immediately indicating the typical behavior of a semiconductor in which the charge carriers drift in opposite directions. As we mentioned before, the electric field promotes the spatial redistribution of ions and vacancies. In fact, measurement of photoluminescence after the removal of the electric field also helps to understand the redistribution and the movement of ions and the non-radiative recombination of the carriers in the traps.[123] A clear elucidation of the mechanism that operates in a LHP layer when voltage is applied across the layer affecting the PL was theoretical and experimentally demonstrated by Bisquert and col. [124] They propose a model based on the modification of the electronic concentration due to the movement of the halide vacancies which migrate and redistribute under applied potential. As we know, these vacancies are non-radiative recombination centers whose spatial distribution is modified in a time scale longer that the characteristic time of electronic migration. From that way, they provide a strong evidence of how the PL decreases as the ionic drift takes place within the film. This phenomenon is analyzed by *in situ* PL microscopy under bias where a sharp dark front moves from one electrode to the other.

3. Conclusions and outlook

While the prospects for LHP playing a key role in future optoelectronic devices are bright, the issue of material instability when interacting with its surroundings will

definitely need to be tackled in the coming years. As evidenced from the results discussed above, instability is not necessarily playing against material performance but a full understanding of its origin is still lacking. Such knowledge will allow exploiting material interaction with its surroundings in the appropriate manner in order to profit from those aspects leading to an improvement of performance.

Despite the consensus achieved on the defect tolerance of lead halide perovskites, where most intrinsic defects lead to electronic states lying either within the valence and conduction bands or close to their edges in the shape of shallow defects, there is still an open debate on their precise origin. Impressive work dealing with their spatial distribution and energetic landscape has shown a complex scenario with disorder extending over several length scales. Identifying the exact chemical nature of such defects as well as its energy and oxidation state will be a key step into understanding the role played by structural disorder in the optoelectronic properties of LHP and guide future processing routes. In this direction, the combination of the above mentioned approaches with ultra-high spatial resolution imaging techniques such as low-dose scanning transmission electron microscopy, where the atomic distribution in a LHP film has been just recently unveiled minimizing material damage, [125] could render a clearer image of structural disorder in these materials.

A more detailed knowledge of the defect structure will benefit other aspects of their photophysical properties such as their interaction with the surrounding atmosphere. In particular unveiling the exact mechanisms behind the photo-induced activation and darkening of their PL in the presence of oxygen could introduce irradiation treatments where the material can be “frozen” at the point where PL activation prevails over material degradation. Intimately linked with this is the instability associated with the

photo-induced ionic migration which adds up to that induced by external electric fields degrading the device performance.

Also related with operational aspects of devices the results discussed dealing with charge contact layers points to interfacial engineering playing a key role in the coming years. Here again, discriminating the type of defects present at the surfaces and grain boundaries of LHP will permit carrying out a design where energetic but also material isolation and defect passivating considerations are taken into account, leading to improved devices.

As mentioned above, synthesis conditions affect the defect structure of materials both within the bulk but also at grain boundaries. Learning on the precise nature of defects and their role on material performance will guide new synthetic approaches which will improve material stability and also end with conflicting reports on issues such as the role of grain boundaries. In this aspect the flexibility introduced by the different established solution process synthetic methods, allowing playing with the precursor ratios but also introducing passivating agents, will be extremely beneficial when combined with additional studies on material formation. Furthermore, more emphasis must be put on the elucidation of the chemical composition of the synthesized perovskites at the microscale. This characterization should be done not only in the fresh prepared materials but also after the interaction with the external factors herein described. Microstructural *in-situ* techniques could supply direct information about the changes when perovskite materials are exposed to electric field, atmosphere or UV-Vis-NIR radiation.

In summary, photophysical properties of LHPs have showed to be strongly linked to the complex interaction of this material with its surroundings. Research efforts aiming at clearly establishing the effect of each external factor on the optoelectronic performance

of perovskites will certainly pay off not only in allowing producing devices with enhanced stability and efficiency, but also to shed light into the photophysics of a fascinating material which is forcing us to revisit many established concepts in semiconductor physics and chemistry.

Acknowledgements

Financial support of the Spanish Ministry of Science and Innovation under grant MAT2017-88584-R (AEI/FEDER, UE) is gratefully acknowledged.

REFERENCES:

[1] A. K. Jena, A. Kulkarni, T. Miyasaka, *Chem. Rev.* **2019**, *119*, 3036.

[2] IEA. *World Energy Outlook 2017* (IEA, Paris, 2017)

[3] Y-H. Kim, J. S. Kim, T-W. Lee, *Adv. Mater.* **2019**, *11*, 1804595.

[4] J. Zhou, J. Huang, *Adv. Sci.* **2018**, *5*, 1700256.

[5] Q. Liao, X. Jin, H. Fu, *Adv. Opt. Mater.* **2019**, *17*, 1900099.

[6] M. Baranowski, P. Plochocka, *Adv. Energy Mater.* **2020**, *11*, 1903659.

[7] S. D. Stranks, G. E. Eperon, G. Grancini, C. Menelaou, M. J. P. Alcocer, T. Leijtens, L. M. Herz, A. Petrozza, H. J. Snaith, *Science* **2013**, *342*, 341.

[8] J. P. Correa-Baena, et al, *Energy Environ. Sci.* **2017**, *10*, 710.

[9] M. A. Green, Y. Jiang, A. M. Soufiani, A. Ho-Baillie, *J. Phys. Chem. Lett.* **2015**, 6, 4774.

[10] H.-H. Fan, S. Adjokatse, H. Wei, J. Yang, G. R. Blake, J Huang, J. Even, M. A. Loi, *Sci. Adv.* **2016**, *2*, e1600534.

[11] S. G. Motti, M. Gandini, A. J. Barker, J. M. Ball, A. R. Srimath Kandada, A. Petrozza, *ACS Energy Lett.* **2016**, *1*, 726.

[12] M. Anaya, J. F. Galisteo-López, M. E. Calvo, J. P. Espinós, H. Míguez, *J. Phys. Chem. Lett.* **2018**, *9*, 3891.

[13] V. D'Innocenzo, A. R. S. Kandada, M. De Bastiani, M. Gandini, A. Petrozza, *J. Am. Chem. Soc.* **2014**, *136*, 17730.

[14] J. F. Galisteo-López, M. Anaya, M. E. Calvo, H. Míguez, *J. Phys. Chem. Lett.* **2015**, *6*, 2200.

[15] Y. Tian, M. Peter, E. Unger, M. Abdellah, K. Zheng, T. Pullerits, A. Yartsev, V. Sundström, I. G. Scheblykin, *Phys. Chem. Chem. Phys.* **2015**, *17*, 24978.

[16] D. Lu, Y. Zhang, M. L. Lai, A. Lee, C. L. Xie, J. Lin, T. Lei, Z. N. Lin, C. S. Kley, J. M. Huang, et al. *Nano Lett.* **2018**, *18*, 6967.

[17] O. D. Miller, E. Yablonovitch, S. R. Kurtz, *IEEE J. Photovoltaics* **2012**, 2, 303.

[18] L. M. Pazos-Outón, T. P. Xiao, E. Yablonovitch, *J. Phys. Chem. Lett.* **2018**, *9*, 1703.

[19] W. Shockley, H. J. Queisser, *J. Appl. Phys.* **1961**, 32, 510.

[20] Y. Liu, Z. Yang, D. Cui, X. Ren, J. Sun, X. Liu, J. Zhang, Q. Wei, H. Fan, F. Yu, et al. *Adv. Mater.* **2015**, *27*, 5176.

[21] A. A. Zhumekenov, M. I. Saidaminov, M. A. Haque, E. Alarousu, S. P. Sarmah, B. Murali, I. Dursun, I.; X.-H. Miao, A. L. Abdelhady, T. Wu, et al. *ACS Energy Lett.* **2016**, *1*, 32.

[22] M. I. Saidaminov, M. A. Haque, J. Almutlaq, S. Sarmah, X. H. Miao, R. Begum, A. A. Zhumekenov, I. Dursun, N. Cho, B. Murali, et al. *Adv. Opt. Mater.* **2017**, *5*, 1600704.

[23] D. W. de Quilettes, S. M. Vorpahl, S. D. Stranks, H. Nagaoka, G. E. Eperon, M. E. Ziffer, H. J. Snaith, D. S. Ginger, *Science* **2015**, *348*, 683.

[24] G. Yin, H. Zhao, H. Jiang, S. Yuan, T. Niu, K. Zhao, Z. Liu, S. Liu, S. *Adv. Funct. Mater.*, **2018**, *28*, 1803269.

[25] W. S. Yang, B.-W. Park, E. H. Jung, N. J. Jeon, Y. C. Kim, D. U. Lee, S. S. Shin, J. Seo, E. K. Kim, J. H. Noh, *Science*, **2017**, *356*, 1376.

[26] S. G. Motti, D. Meggiolaro, S. Martani, S. Sorrentino, A. J. Barker, F. De Angelis, A. Petrozza, *Advanced Materials* **2019**, 31, 1901183.

[27] N. K. Noel, A. Abate, S. D. Stranks, E. Parrott, E. Burlakov, A. Goriely, H. J. Snaith, *ACS Nano* **2014**, *8*, 9815.

[28] M. Abdi-Jalebi, Z. Andaji-Garmaroudi, S. Cacovich, C. Stavrakas, B. Philippe, J. M. Richter, M. Alsari, E. P. Booker, E. M. Hutter, A. J. Pearson, S. Lilliu, T. J. Savenije, H. Rensmo, G. Divitini, C. Ducati, R. H. Friend, S. D. Stranks, *Nature* **2018**, *555*, 497.

[29] Q. Jiang, Y. Zhao, X. Zhang, X. Yang, Y. Chen, Z. Chu, Q. Ye, X. Li, Z. Yin, J. You, *Nat. Photonics* **2019**, *13*, 460.

[30] T. A. S. Doherty, et al. *Nature* **2020**, *580*, 360.

[31] Z. Ni, C. Bao, Y. Liu, Q. Jiang, W.-Q. Wu, S. Chen, X. Dai, B. Chen, B. Hartweg, Z. Yu, Z. Holman, J. Huang, *Science* **2020**, *367*, 1352.

[32] T. W. Jones, et al. *Energy Environ. Sci.* **2019**, *12*, 596.

[33] J. Kang, L.-W. Wang, *J. Phys. Chem. Lett.* **2017**, *8*, 489.

[34] Y. Li, C. Zhang, X. Zhang, D. Huang, Q. Shen, Y. Cheng, W. Huang, *Appl. Phys. Lett.* **2017**, *111*, 162106.

[35] J.-S. Park, J. Calbo, Y.-K. Jung, L. D. Whalley, A. Walsh, *ACS Energy Lett.* **2019**, *4*, 1321.

[36] S. T. Brinck, F. Zaccaria, I. Infante, *ACS Energy Lett.* **2019**, *4*, 2739.

[37] F. Liu, Y. Zhang, C. Ding, S. Kobayashi, T. Izuishi, N. Nakazawa, T. Toyoda, T. Ohta, S. Hayase, T. Minemoto, K. Yoshino, S. Dai, Q. Shen, *ACS Nano* **2017**, *11*, 10373.

[38] Y. Yuan, J. Huang, *Acc. Chem. Res.* **2016**, *49*, 286.

[39] R. S. Sánchez, V. González-Pedro, J.-W. Lee, N.-G. Park, Y. S. Kang, I. Mora-Sero, J. Bisquert, *J. Phys. Chem. Lett.* **2014**, *5*, 2357.

[40] S. D. Stranks, V. M. Burlakov, T. Leijtens, J. M. Ball, A. Goriely, H. J. Snaith, *Phys. Rev. Appl.* **2014**, *2*, 034007.

[41] D. W. DeQuilettes, W. Zhang, V. M. Burlakov, D. J. Graham, T. Leijtens, A. Osherov, V. Bulovic, H. J. Snaith, D. S. Ginger, S. D. Stranks, *Nat. Commun.* **2016**, *7*, 11683.

[42] D. W. DeQuilettes, S. Koch, S. Burke, R. K. Paranji, A. J. Shropshire, M. E. Ziffer, D. S. Ginger, *ACS Energy Lett.* **2016**, 1, 438.

[43] J. F. Galisteo-López, Y. Li, H. Míguez, *J. Phys. Chem. Lett.* **2016**, *7*, 5227.

[44] H.-H. Fang, F. Wang, S. Adjokatse, N. Zhao, M. A. Loi, *Adv. Funct. Mater.* **2016**, *26*, 4653.

[45] R. Brenes, D. Guo, A. Osherov, N. K. Noel, C. Eames, E. M. Hutter, S. K. Pathak, F. Niroui, R. H. Friend, M. S. Islam, H. J. Snaith, V. Bulović, T. Savenije, S. D. Stranks, *Joule* **2017**, *1*, 155.

[46] R. Brenes, C. Eames, V. Bulovic, M. S. Islam, S. D. Stranks, *Adv. Mater.* **2018**, *30*, 1706208.

[47] J. F. Galisteo-López, M. E. Calvo, H. Míguez, *ACS Appl. Energy. Mater.*, **2019**, *2*, 6967.

[48] N. Phung, A. Al-Ashouri, S. Meloni, A. Mattoni, S. Albrecht, E. L. Unger, A. Merdasa, A. Abate, *Adv. Energy Mater.*, **2020**, *10*, 1903735.

[49] E. Mosconi, D. Meggiolaro, H. J. Snaith, S. D. Stranks, F. De Angelis, *Energy Environ. Sci.*, **2016**, *9*, 3180.

[50] M. Saliba, T. Matsui, J.-Y. Seo, K. Domanski, J. P. Correa-Baena, M. K. Nazeeruddin, S. M. Zakeeruddin, W. Tress, A. Abate, A. Hagfeldt, M. Grätzel, *Energy Environ. Sci.* **2016**, *9*, 1989.

[51] M. I. Saidaminov, J. Kim, A. Jain, R. Quintero-Bermudez, H. Tan, G. Long, F. Tan, A. Johnston, Y. Zhao, O. Voznyy, E. H. Sargent, *Nat. Energy.* **2018**, *3*, 648.

[52] D. W. Ferdani, S. R. Pering, D. Ghosh, P. Kubiak, A. B. Walker, S. E. Lewis, A. L. Johnson, P. J. Baker, M. S. Islam, P. J. Cameron, *Energy Environ. Sci.* **2019**, *12*, 2264.

[53] E. T. Hoke, D. J. Slotcavage, E. R. Dohner, A. R. Bowring, H. I. Karunadasa, M. D. McGehee, *Chem. Sci.* **2015**, *6*, 613.

[54] G. F. Samu, C. Janáky, P. V. Kamat, *ACS Energy Lett.* **2017**, *2*, 1860.

[55] R. A. Belisle, K. A. Bush, L. Bertoluzzi, A. Gold-Parker, M F. Toney, M. D. McGehee, *ACS Energy Lett.* **2018**, *3*, 2694.

[56] M. Hu, C. Bi, Y. Yuan, Y. Bai, J. Huang, *Adv. Sci.* **2016**, *3*, 1500301.

[57] X. Tang, M. van den Berg, E. Gu, A: Horneber, G. J. Matt, A. Osvet, A. J. Meixner, D. Zhang, C. J. Brabec, *Nano Lett.* **2018**, *18*, 2172.

[58] Y. Zhou, Y.-H. Jia, H.-H. Fang, M. A. Loi, F.-Y. Xie, L. Gong, M.-C. Qin, X.-H. Lu, C.-P. Wong, N. Zhao, *Adv. Funct. Mater.* **2018**, *28*, 1803130.

[59] Z. B. Yang, A. Rajagopal, S. B. Jo, C. C. Chueh, S. Williams, C. C. Huang, J. K. Katahara, H. W. Hillhouse, A. K. Y. Jen, *Nano Lett.* **2016**, *16*, 7739.

[60] A. J. Barker, A. A. Sadhanala, F. Deschler, M. Gandini, S. P. Senanayak, P. M. Pearce, E. Mosconi, A. J. Pearson, Y. Wu, Y.; A. R: S. Kandada, *ACS Energy Lett.* **2017**, *2*, 1416.

[61] S. J. Yoon, M. Kuno, P. V. Kamat, *ACS Energy Lett.* **2017**, *2*, 1507.

[62] R. G. Balakrishna, S. M. Kobosko, P. V. Kamat, *ACS Energy Lett.* **2018**, *3*, 2267.

[63] A. Ruth, M. C. Brennan, S. Draguta, Y. V. Morozov, M. Zhukovskyi, B. Janko, P. Zapol, M. Kuno, *ACS Energy Lett.* **2018**, *3*, 2321.

[64] A. J. Knight, A. D. Wright, J. B. Patel, D. P. McMeekin, H. J. Snaith, M. B. Johnston, L. M. Herz, *ACS Energy Lett.* **2019**, *4*, 75.

[65] D. O. Tiede, J. F. Galisteo-López, M. E. Calvo, H. Míguez, *J. Phys. Chem. Lett.* **2020**, *11*, 4911.

[66] A. J. Knight, L. M. Herz, *Energy Environ. Sci.*, **2020**, *13*, 2024.

[67] J. L. Pankove, *Optical Processes in Semiconductors*; Dover Publications Inc.: New York, 1975.

[68] N. Aristidou, I. Sanchez-Molina, T. Chotchuangchutchaval, M. Brown, L. Martinez, T. Rath, S. A. Haque, *Angew. Chem., Int. Ed.* **2015**, *54*, 8208.

[69] L. Zhang, P. H. L. Sit, *J. Mater. Chem. A* **2017**, *5*, 9042.

[70] N. Aristidou, C. Eames, I. Sanchez-Molina, X. Bu, J. Kosco, M. S. Islam, S. A. Haque, *Nat. Commun.* **2017**, *8*, 15218.

[71] A. Senocrate, T. Acartürk, G. Y. Kim, R. Merkle, U. Starke, M. Grätzel, J. Maier, *J. Mater. Chem. A* **2018**, *6*, 10847.

[72] J. Huang, S. Tan, P. D. Lund, P. D.; Zhou, H. Impact of H_2O on Organic−Inorganic Hybrid Perovskite Solar Cells. *Energy Environ. Sci.* **2017**, *10*, 2284−2311.

[73] E. Mosconi, J. M. Azpiroz, F. De Angelis, *Chem. Mater.* **2015**, *27*, 4885.

[74] Y.-B. Lu, W.-Y. Cong, C. Guan, H. Sun, Y. Xin, K. Wang, S. Song, *J. Mater. Chem. A* **2019**, *7*, 27469.

[75] Z. Andaji-Garmaroudi, M. Anaya, A. J. Pearson, S. D. Stranks, *Adv. Energy Mater.* **2019**, *10*, 1903109.

[76] X. Feng, H. Su, Y. Wu, H. Wu, J. Xie, X. Liu, J. Fan, J. Dai, Z. He, *J. Mater. Chem. A* **2017**, *5*, 12048.

[77] D. Lu, Y. Zhang, M. L. Lai, A. Lee, C. L. Xie, J. Lin, T. Lei, Z. N. Lin, C. S. Kley, J. M. Huang, et al. *Nano Lett.* **2018**, *18*, 6967.

[78] J. He, W. H. Fang, R. Long, O. V. Prezhdo, *J. Am. Chem. Soc.* **2019**, *141*, 5798.

[79] D. Meggiolaro, E. Mosconi, F. De Angelis, *ACS Energy Lett.* **2017**, *2*, 2794.

[80] J. S. W. Godding, A. J. Ramadan, Y.-H. Lin, K. Schutt, H. J. Snaith, B. Wenger, *Joule* **2019**, *3*, 2716.

[81] Z. Hu, Z. Liu, L. K. Ono, M. Jiang, S. He, D.-Y. Son, Y. Qi, *Adv. Energy Mater.* **2020**, *11*, 2000908.

[82] Y. Wang, Y. et al. *Science* **2019**, *365*, 591.

[83] S. C. Liu, Z. Li, Y. Yang, X. Wang, Y. X. Chen, D. J. Xue, J. S. Hu, *J. Am. Chem. Soc.* **2019**, *141*, 18075.

[84] D. Lu, Y. Zhang, M. L. Lai, A. Lee, C. L. Xie, J. Lin, T. Lei, Z. N. Lin, C. S. Kley, J. M. Huang, et al. *Nano Lett.* **2018**, *18*, 6967.

[85] L. Qiao, R. Long, W. H. Fang, *J. Phys. Chem. Lett.* **2019**, *10*, 5499.

[86] I. C. Smith, E. T. Hoke, D. Solis-Ibarra, M. D. McGehee, H. I. A. Karunadasa, *Angew. Chem., Int. Ed.***2014**, *53*, 11232.

[87] J. Cho, J. T. DuBose, A. N. T. Le, P. V. Kamat, *ACS Mater. Lett.* **2020**, *2* , 565.

[88] Y. Song, W. Liu, Y. Qin, X. Han, W. Li, X. Li, H. Long, D. Li, K. Wang, B. Wang, P. Lu, *Adv. Optical Mater.* **2020**, *8*, 1901695.

[89] A number of recent review articles have thoroughly described the interaction of LHP surfaces with adjacent CTLs: A. Rajagopal, K. Yao, A. K. Jen, *Adv. Mater.* **2018,** *30*, 1800455; P. Schulz, D. Cahen, A. Kahn, *Chem. Rev.* **2019**, *119*, 3349.

[90] Y. Lin, L. Shen, J. Dai, Y. Deng, Y. Wu, Y. Bai, X. Zheng, J. Wang, Y. Fang, H. Wei, W. Ma, X. C. Zeng, X. Zhan, J. Huang, *Adv. Mater.* **2017**, *29*, 1604545.

[91] H. Chen, W. Fu, C. Huang, Z. Zhang, S. Li, F. Ding, M. Shi, C.-Z. Li, A. K.-Y. Jen, H. Chen, *Adv. Energy Mater.* **2017**, 1700012.

[92] Y. Shao, Z. Xiao, C. Bi, Y. Yuan, J. Huang, *Nature Comm.* **2014**, *5*, 5784.

[93] P.-W. Liang, C.-C. Chueh, S. T. Williams, A. K.-Y. Jen, *Adv. Energy Mater.* **2015**, *5*, 1402321.

[94] A. J. Pearson, G. E. Eperon, P. E. Hopkinson, S. N. Habisreutinger, J. T.-W. Wang, H. J. Snaith, N. C. Greenham, *Energy Mater.* **2016**, *6*, 1600014.

[95] D. Bryant, N. Aristidou, S. Pont, I. Sanchez-Molina, T. Chotchunangatchaval, S. Wheeler, J. R. Durrant, S. A. Haque, *Energy Environ. Sci.* **2016**, *9*, 1655.

[96] H. Back, G. Kim, J. Kim, J. Kong, T. K. Kim, H. Kang, H. Kim, J. Lee, S. Lee, K. Lee, *Energy Environ. Sci.* **2016**, *9*, 1258.

[97] C. Aranda, J. Bisquert, A. Guerrero, *J. Chem. Phys.* **2019**, *151*, 124201.

[98] A. F. Akbulatov, L. A. Frolova, M. P. Griffin, I. R. Gearba, A. Dolocan, D. Vanden Bout, S. Tsarev, E. A. Katz, A. F. Shestakov, K. J. Stevenson, P. A. Troshin, *Adv. Energy Mater.* **2017**, *7*, 1700476.

[99] K. Domanski, J. P. Correa-Baena, N. Mine, M. K. Nazeeruddin, A. Abate, M. Saliba, W. Tress, A. Hagfeldt, M. Grätzel, *ACS Nano* **2016**, *10*, 6306.

[100] T. Leijtens, G. E. Eperon, S. Pathak, A. Abate, M. M. Lee, H. J. Snaith, *Nat. Commun.* **2014**, *4*, 2885.

[101] J. Yang, B. D. Siempelkamp, E. Mosconi, F. De Angelis, T. L. Kelly, *Chem. Mater.* **2015**, *27*, 4229.

[102] J. A. Christians, P. Schulz, J. S. Tinkham, T. H. Schloemer, S. P. Harvey, B. J. Tremolet de Villers, A. Sellinger, J. J. Berry, J. M. Luther, *Nat. Energy* **2018**, *3*, 68.

[103] J. Yin, J. Cao, X. He, S. Yuan, S. Sun, J. Li, N. Zheng, L. Lin, *J. Mater. Chem. A* **2015**,*3*, 16860.

[104] T. Leijtens, G. E. Eperon, S. Pathak, A. Abate, M. M. Lee, H. J. Snaith, *Nat. Commun.* **2013**, *4*, 2885.

[105] B. Roose, J. P. Baena, K. C. Gödel, M. Graetzel, A: Hagfeldt, U. Steiner, A. Abate, *Nano Energy* **2016**, *30*, 517.

[106] J. Xie, X. Yu, J. Huang, X. Sun, Y. Zhang, Z. Yang, M. Lei, L. Xu, Z. Tang, C. Cui, P. Wang, D. Yang, *Adv. Sci.* **2017**, *4*, 1700018

[107] Y. Sun, X. Fang, Z. Ma, L. Xu, Y. Lu, Q. Yu, N. Yuan, J. Ding, *J. Mater. Chem. C* **2017**, *5*, 8682.

[108] Q. Chen, H. Zhou, T. B. Song, S. Luo, Z. Hong, H. S. Duan, L. Dou, Y. Liu, Y. Yang, *Nano Lett.* **2014**, *14*, 4158.

[109] T. J. Jacobsson, J.-P. Correa-Baena, E. Halvani Anaraki, B. Philippe, S. D. Stranks, M. E. F. Bouduban, W. Tress, K. Schenk, J. Teuscher, J.-E. Moser, H. Rensmo, A. Hagfeldt, *J. Am. Chem. Soc.* **2016**, *138*, 10331.

[110] Y. C. Kim, N. J. Jeon, J. H. Noh, W. S. Yang, J. Seo, J. S. Yun, A. Ho-Baillie, S. Huang, M. A. Green, J. Seidel, T. K. Ahn, S. I. Seok, *Adv. Energy Mater.* **2016**, *6*, 1502104

[111] A. Merdasa, A. Kiligaridis, C. Rehermann, M. Abdi-Jalebi, J. Stöber, B. Louis, M. Gerhard, S. D. Stranks, E. L. Unger, I. G. Scheblykin, *ACS Energy Letters* **2019,** *4*,1370

[112] Y. Chen, Q. Meng, Y. Xiao, X. Zhang, J. Sun, C. B. Han, H. Gao, Y. Zhang, Y. Lu, H. Yan, *ACS Appl. Mater. Interfaces* **2019**, *11*, 44101

[113] J. Barbé, M. Newman, S. Lilliu, V. Kumar, H. Ka Hin Lee, C. Charbonneau, C. Rodenburg, D. Lidzey, W. Chung Tsoi, *J. Mater. Chem. A*, **2018**, *6*, 23010.

[114] K. Lin, J. Xing, L. N. Quan, F. P. G. de Arquer, X. Gong, J. Lu, L. Xie, W. Zhao, D. Zhang, C. Yan, W. Li, X. Liu, Y. Lu, J. Kirman, E.H. Sargent, Q. Xiong, Z. Wei, Z. *Nature* **2018**, *562*, 245.

[115] M. Abdi-Jalebi, Z. Andaji-Garmaroudi, S. Cacovich, C. Stavrakas, B. Philippe, J. M. Richter, M. Alsari, E. P. Booker, E. M. Hutter, A. J. Pearson, S. Lilliu, T. J. Savenije, H. Rensmo, G. Divitini, C. Ducati, R. H. Friend, S. D. Stranks, *Nature* **2018**, *555*, 497.

[116] Y. Guo, K. Shoyama, W. Sato, E. Nakamura, *Adv. Energy Mater.* **2016**, *6*, 1502317

[117] Y. Zong, Y. Zhou, Y. Zhang, Z. Li, L. Zhang, M.-G. Ju, M. Chen, S. Pang, X. C. Zeng, N. P. Padture, *Chem* **2018**, *4*, 1404

[118] S. Bae, S. Kim, S.-W. Lee, K. J. Cho, S. Park, S. Lee, Y. Kang, H.-S. Lee and D. Kim, *J. Phys. Chem. Lett.*, **2016**, *7*, 3091.

[119] T. Leijtens, E. T. Hoke, G. Grancini, D. J. Slotcavage, G. E. Eperon, J. M. Ball, M. De Bastiani, A. R. Bowring, N. Martino, K. Wojciechowski, M. D. McGehee, H. J. Snaith, A. Petrozza, *Adv. Energy Mater.* **2015**, *5*, 1500962.

[120] J. Wu, J. Wu, Y. Li, S. Tan, B. Yu, H. Li, Y. Li, J. Shi, H. Wu, Y. Luo, D. Li, Q. Meng, *ACS Appl. Mater. Interfaces* **2020**, *12*, 27258.

[121] K. Domanski, E. A. Alharbi, A. Hagfeldt, M. Grätzel, W. Tress, *Nat. Energy*, **2018**, *3*, 61.

[122] W. Nie, J.-C. Blancon, A. J. Neukirch, K. Appavoo, H. Tsai, M. Chhowalla, M. A. Alam, M. Y. Sfeir, C. Katan, J. Even, *Nat. Commun.* **2016**, *7*, 11574

[123] T. Leijtens, A. R. Srimath Kandada, G. E. Eperon, G. Grancini, V. D'Innocenzo, J. M. Ball, S. D. Stranks, H. J. Snaith, A. Petrozza, *J. Am. Chem. Soc.* **2015**, *137*, 15451

[124] C. Li, A. Guerrero, S. Huettner, J. Bisquert, *Nat. Commun.* **2018**, *9*, 5113

[125] M. U. Rothmann, J. S. Kim, J. Borchert, K. B. Lohmann, C. M. O'Leary, A. A. Sheader, L. Clark, H. J. Snaith, M. B. Johnston, P. D. Nellist, L. M. Herz, Science **2020**, *370*, 548.